UDC 539.4

Smooth Particle Hydrodynamics-Based Characteristics of a Shaped Jet from Different Materials

J. P. Yin,[1] Z. X. Shi, J. Chen, B. H. Chang, and J. Y. Yi

School of Mechatronic Engineering, North University of China, Taiyuan, China

[1] yjp123@nuc.edu.cn

The liner material is one of the key factors in the design of armor-piercing ammunition that effect the penetration efficiency. The performance of a shaped jet formed by the charge liner is determined by different properties of the material under the blasting action, in particular for the target with explosive reactive armor, which diminishes the penetration power by dispersing the shaped jet. The performance of shaped jet elements from different materials is studied, AUTODYN finite element software and smooth particle hydrodynamics method are employed to simulate the formation of shaped jet elements from the three materials: Cu, PTFE, and PTFE/Cu and their penetration into target plates, which was verified in the experiment. A shaped jet for a Cu liner is shown to be formed under the action of a detonation wave, while PTFE and PTFE/Cu materials generate a dispersive particle jet. The head velocity of a Cu jet is found to be the lowest, the penetration depth is the deepest, and the penetration hole size is the smallest; the velocity of a PTFE particle jet is the highest and the penetration depth is the shallowest, the penetration hole size takes the mid-position; the head velocity and penetration depth of a PTFE/Cu jet take the mid-position, while the penetration hole is the largest. The PTFE/Cu jet possesses higher penetration performance as compared to the PTFE jet, and its hole-opening capability is improved as compared to the Cu jet.

Keywords: particle jet, smooth particle hydrodynamics, explosive reactive armor, liner material, polytetrafluoroethylene (PTFE).

Introduction. Over the years, armoured and anti-armor technologies have been developing against each other. Currently, among the artillery shells, rockets and missile warheads, shaped charge is one of the effective ways to deal with the damage of advanced protective armor. In recent years, several local wars have shown that armored vehicles and tanks are still the main assault forces on the ground battlefield, and urban warfare has become more and more common. So it is very important to destroy the enemy's armored vehicles protected by reactive armor and avoid the humanitarian condemnation caused by unnecessary casualties cause to civilians [1]. In view of this background, how to improve the comprehensive penetration performance of tandem anti-armor ammunition is one of the hot spots in the world [2]. The literature shows that the key to solve this problem lies in the control of the length, shape, quality, energy and so on of the damage elements, and the choice of the liner material is very crucial, the suitable materials can improve the comprehensive penetration performance of the damage elements in varying degrees [3–5]. At present, the traditional shaped charge uses metal, metal alloy material and large-density material to make a liner, which can form a certain length of continuous and stable damage element, which has the advantages of large impact force and large penetration depth to the target, but it has some disadvantages such as weak reaming ability, small aperture of armor breaking and limited killing power. At present, the design requirement of the tandem warhead of the new anti-explosive reaction armor is to improve the reaming capacity of the damage elements under the condition of ensuring a certain penetration depth, so as to open up a channel for the target of subsequent damage elements to penetrate. Therefore, the use of low density materials as shaped charge material has become one of the main research directions of anti-armor ammunition [6, 7].

Smooth particle hydrodynamics (SPH) is a mesh-free particle method, which not only has the advantages of Lagrange method to calculate and describe the interface of matter accurately, but also has the advantages of meshless method, it is applicable to the calculation of various problems with large fluid deformation and moving boundaries [8]. Currently, particle jet has been carried out at home and abroad: König and Mostert [9] form a particle jet with a polycarbonate material liner; Cornish et al. [10] show that the penetration effect of particle jet is mainly affected by the particle jet shape and velocity; Li et al. [11, 12] put forward the penetration model of particle jet, which makes up for the deficiency of classical theory that the penetration depth of particle jets cannot be calculated. However, most scholars mainly study particle jets theoretically and experimentally, and few do numerical simulation researches. It is obvious that numerical simulation of shaped particle jet is a difficult point in the field of simulation. When the Lagrangian finite element method is used to simulate the formation process of particle jet, a series of problems such as large mesh distortion and slip surface treatment will occur, eventually leading to the decrease of calculation accuracy and even the final failure calculation is caused. The Euler method does not have the problem of large mesh distortion, but it is difficult to accurately describe all kinds of interfaces [13–15]. In this paper, Cu, PTFE and PTFE/Cu liners are taken as the research objects. Based on SPH algorithm, numerical simulation and experimental verification of particle jets forming and penetrating target plate with different materials are carried out to study the forming performance and penetration performance of particle jet with different materials under explosive loading, so as to provide a reference for the design of the front-stage of the tandem anti-armor charge.

1. **Finite Element Model of Particle Jets Forming with Different Materials**.

1.1. ***Geometric Model and Finite Element Model***. In this paper, a 40 mm caliber was used to form the damage elements to penetrate 45# steel target plate. The shaped charge structure was made of conical charge liner with equal wall thickness, and the top of the cone was treated with a round angle. The initial parameters: the liner cone angle was 55°, the charge height was 40 mm, the charge mass was 60 g, and the blast height was 130 mm. In order to verify the damage performance of the PTFE/Cu jet damage element better, the same shaped charge structure was designed to study the formation of jet damage element and penetration of 45# steel target by Cu, PTFE, and PTFE/Cu liners, respectively. The wall thickness of Cu charge liner was 1.1 mm, PTFE and PTFE/Cu charge liner was 3.5 mm. Because of the large material deformation when the charge explosive collapsed the liner, the shape charge adopted the Eulerian algorithm to deal with the problem of large deformation, and the target plate adopted the Lagrangian algorithm. The two algorithms were coupled by fluid-solid coupling. The finite element models of the shape charges forming particle jets and penetrating the target plate are shown in Fig. 1.

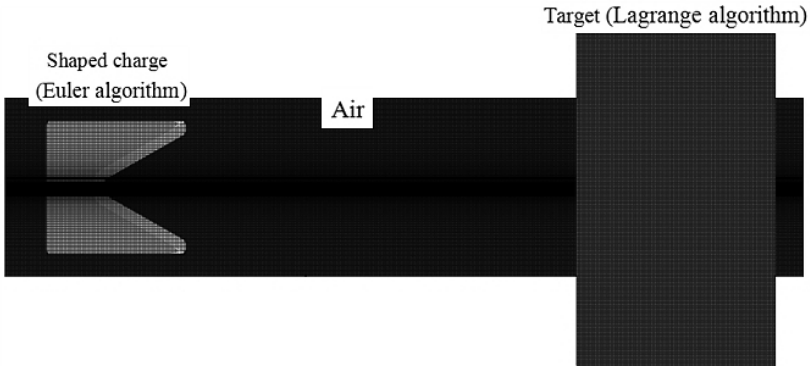

Fig. 1. Particle jet forming and penetrating target plate finite element model.

1.2. ***Material Models and Parameters***. The liner materials used in the numerical simulation were Cu, PTFE and PTFE/Cu, and the target material was 45# steel, the charge was B charge. The constitutive relations and parameters of the main materials are given in Tables 1 and 2, respectively.

Among them, ρ_0 is density, D is B charge detonation velocity, A, B, R_1, R_2, and ω are the explosion parameters, E_0 is C-J internal energy, and P_{C-J} is C-J pressure under dynamic test.

Table 1

Constitutive Relations and Parameters of Main Materials

Material	Density (g/cm^3)	State equation	Strength model	
			Shear modulus (GPa)	Yield stress (MPa)
Cu	8.93	Shock	46.00	90
PTFE	2.16	Shock	2.33	50
PTFE/Cu	3.05	Shock	1.37	46
45# steel	7.85	Linear	81.80	352

Table 2

Basic Parameters of Shape Charge

ρ_0, g/cm^3	D, km/s	A, MPa	B, MPa	R_1	R_2	ω	E_0, kJ/m^3	P_{C-J}, GPa
1.717	7.98	524,230	7678	4.2	1.1	0.34	$8.5 \cdot 10^6$	29.5

2. **Different Materials Particle Jets Forming Performance**.

2.1. ***Forming Process Numerical Simulation***. By means of charge center initiation, the process of particle jets forming of three different materials is shown in Figs. 2–4. It can be seen that three different materials of particle jets forming process includes four stages: shaped charge detonation process, charge liner collapse, particle jet initial formation and particle jet stretching. The numerical simulation results showed that the detonation wave reached the top of the charge liner at the beginning of 2 μs from the detonating shaped charge and began to act on the liner to make it crush and shape, which caused the charge liner to be completely crushed when it collapsed into 5 μs. At 5 μs, the liner was completely crushed, and the particles of the charge shell were squeezed toward the center at a high speed after compression, and the initial jet and pestle were formed after the collision occur on the axis. 5~15 μs was the key time for jet formation. In this period, the crushed powder particles would converge on the axis to form a jet and a pestle. At 20 μs, the basic shape of the jet had been formed, and then the three kinds of jets had a slight difference. The head expansion of the PTFE jet and the PTFE/Cu jet appeared over time, and the particle of the jet material produced radial motion, the diameter gradually became larger and finally formed a dispersed particle jet, while the Cu particle jet was elongated and thinned over time, resulting in necking and fracture phenomena, but the particle jet condensed in shape.

2.2. ***Forming Performance Analysis***. In order to study the formability of different materials' particle jets, numerical simulation method was used to comparatively analyze the forming process of Cu particle jet, PTFE particle jet and PTFE/Cu particle jet. The jet head velocity of three kinds of materials is shown in Fig. 5.

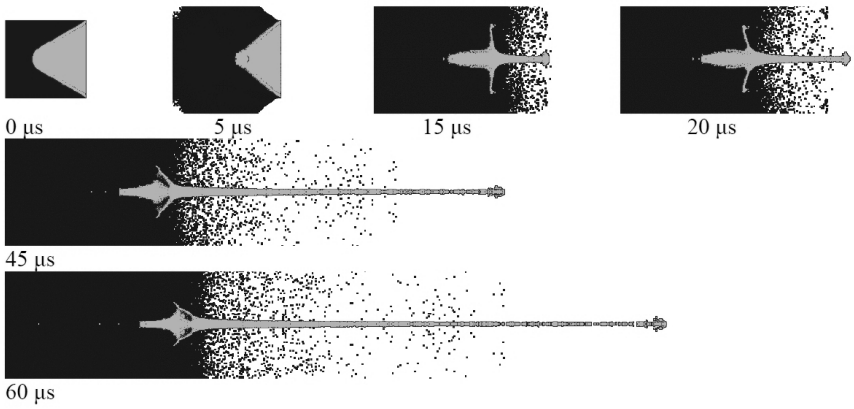

Fig. 2. Cu particle jet forming process diagram.

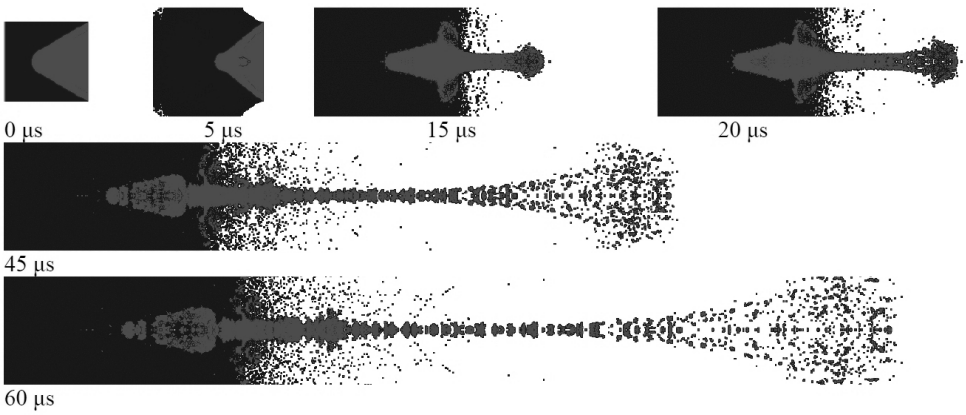

Fig. 3. PTFE particle jet forming process diagram.

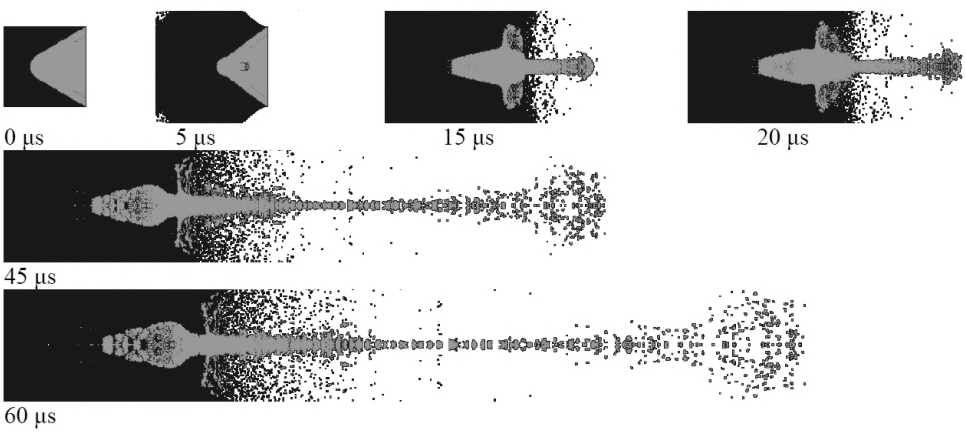

Fig. 4. PTFE/Cu particle jet forming process diagram.

It can be seen from the variation curves of velocity and time of three kinds of particle jet head that when the detonation wave of the explosive was transmitted to the charge liner,

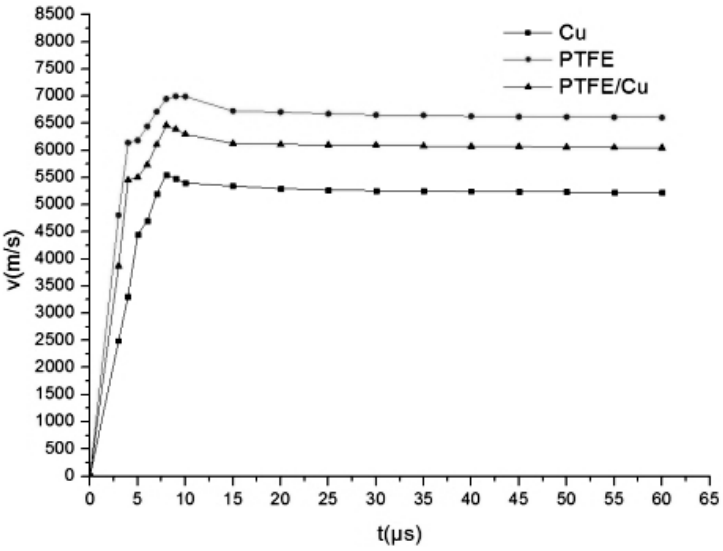

Fig. 5. Head velocity variation curve of three kinds of particle jet.

the liner was quickly crushed to form the particle jet head. And with the continuous action of detonation wave pressure, the material and energy of the liner flowed into the particle jet continuously, particle jet head continued to accelerate until it reached the maximum velocity, the maximum flow head velocity of PTFE particle jet reached 6998 m/s at 9 μs, and that of modified PTFE particle jet head reached the maximum value of 6463 m/s at 8 μs, the Cu particle jet head velocity reached a maximum of 5554 m/s at 8 μs. After that, the effect of detonation wave decreased and with the decreasing of material and energy inflow. The velocity of particle jet head gradually decreased, and finally tended to stabilize. At 60 μs, the head velocity of PTFE particle jet was 6607 m/s, PTFE/Cu particle jet head velocity was 6463 m/s, Cu particle jet head velocity was 5554 m/s. The head velocity of PTFE/Cu was lower than that of PTFE, with a small decreasing which was beneficial to its penetrating ability.

2.3. ***Forming Experimental Verification***. In the experiment, 40 mm shell free shaped charge was used, and the combination of two pulse X-ray machines of 450KV produced by HP company was used. The two pulsed X-ray tubes were arranged in 45° confluence, and the shaped charge was arranged vertically, and ensured that the particle jet after forming could pass through the two X-ray tube sink axis. By setting different light time of two pulse X-ray machines, two X-ray photographs at different times can be obtained by one test [16].

X-ray experiments on the particle jets forming process of Cu, PTFE, PTFE/Cu liners were carried out, and the morphologies of the three materials particles were observed as shown in Fig. 6. By comparing the observed jet morphologies with the simulation results, it was found that all three materials (Cu, PTFE, and PTFE/Cu) could form a good-shaped particle jet damage element. The Cu particle jet was compact, the PTFE particle jet was evacuated, while the diameter of PTFE/Cu particle jet was significantly larger than those of others. The experimental results were in good agreement with the numerical simulations. In addition, it can be seen from the clarity comparison of Fig. 6a–c that the Cu particle jet is most clearly followed by the PTFE/Cu particle jet, and the PTFE particle jet is the clearest since the Cu particle jet density is much larger than the density of the protective plate density of X-ray film. While the PTFE/Cu particle jet density is similar to that of the protective plate of X-ray film, and the sharpness is reduced accordingly.

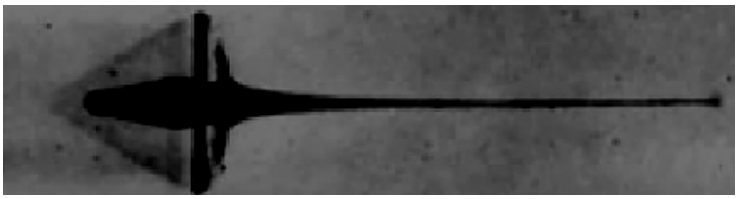

a

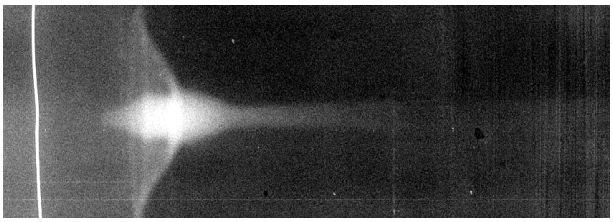

b

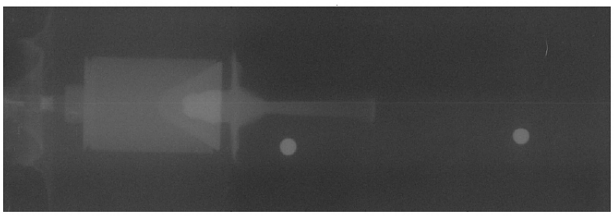

c

Fig. 6. Test results of damage elements forming of different materials: particle jet formation of Cu liner at 18.6 μs (a), PTFE liner at 20 μs (b), and PTFE/Cu liner at 20 μs (c).

3. **Study on Penetration Performance of Particles with Different Materials**.

3.1. ***Penetration Process Numerical Simulation***. In order to further study the penetration ability of modified PTFE particle jet, numerical simulation method was used to simulate the Cu particle jet, PTFE particle jet, and PTFE/Cu particle jet penetrating 45# steel targets in Figs. 7–9.

The process of Cu particle jet penetrating the target plate is depicted in Fig. 7. Starting from detonating shape charge, the head of Cu particle jet destructive element started to penetrate 45# steel target plate at the speed of 4743 m/s at the time of 31 μs. After the penetration of Cu particle jet for 50 μs, the penetration depth reached 69 mm. As time goes on, after 40 μs penetration time, penetration depth increased by only 22 mm and reached 91 mm, the penetration velocity of the target plate significantly decreased, and the Cu particle jet appeared obvious accumulation phenomenon. At this time, the maximum velocity of Cu particle jet was 1878 m/s, but it can also slowly penetrated the target plate. After 25 μs, the remaining velocity was 712.5 m/s, and the deposition of Cu particle jet became more serious and their penetration ability was almost lost. At this time, the penetration depth of Cu damage element reached 98.4 mm.

The process of PTFE particle jet penetrating the target plate is shown in Fig. 8. From the beginning of charge detonation warhead, the PTFE particle jet was 6 μs earlier than Cu particle jet damage element. At 25 μs, the PTFE particle jet began to penetrate the target plate at 5575 m/s velocity. The penetration depth reached 21 mm after the PTFE particle jet penetrates the target plate 30 μs. At this time, there was an obvious jet accumulation phenomenon, but the maximum velocity of the damage element was 2538 m/s, and the remaining velocity was higher. Therefore, the damage element continued to penetrate the target, and after 30 μs penetration, the penetration depth was increased only by 1.1 to

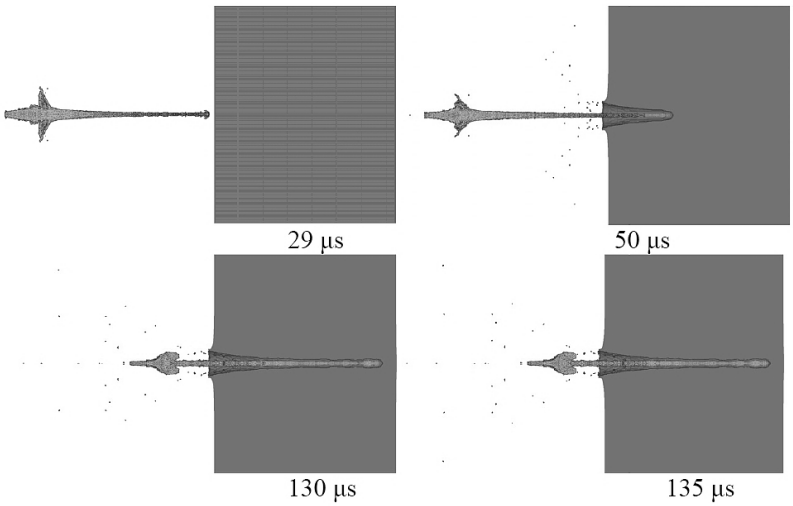

Fig. 7. The process of Cu particle jet penetrating the target plate.

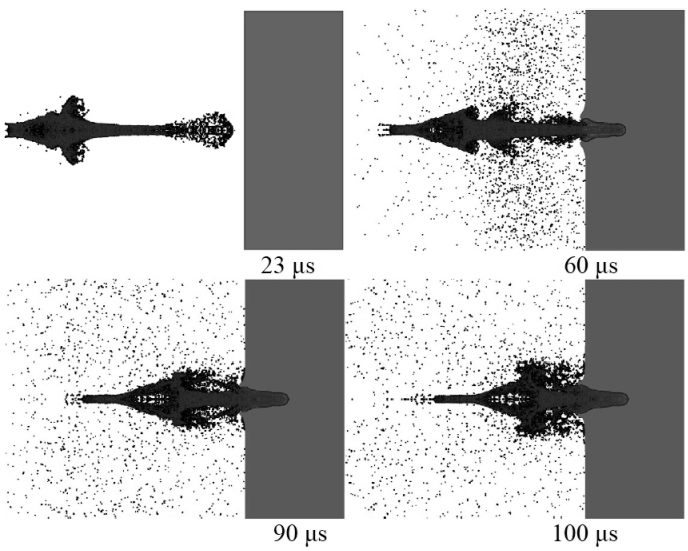

Fig. 8. The process PTFE particle jet penetrating the target plate.

22.1 mm. PTFE particle jet damage element almost lost penetration ability. Because the PTFE head diameter was larger than that of Cu particle jet, and the accumulation phenomenon of perforation in particle jet was more obvious, so the perforation diameter of the PTFE particle jet reached 17.4 mm, which was 7.2 mm higher than that of the Cu particle jet. The maximum penetration depth of PTFE particle jet damage element was 22.1 mm.

The process of PTFE/Cu particle jet penetrating the target plate is shown in Fig. 9. From the start of detonation shape charge, the PTFE/Cu particle jet damage element was 2 μs later than the PTFE particle jet damage element. At the time of 27 μs, the PTFE/Cu particle jet started to penetrate the target plate at a speed of 5263 m/s. And after 33 μs, the penetration depth reached 27 mm, when the PTFE/Cu particle jet began to pile up in the channel of the target plate, but the highest velocity of the damage element was 1748 m/s,

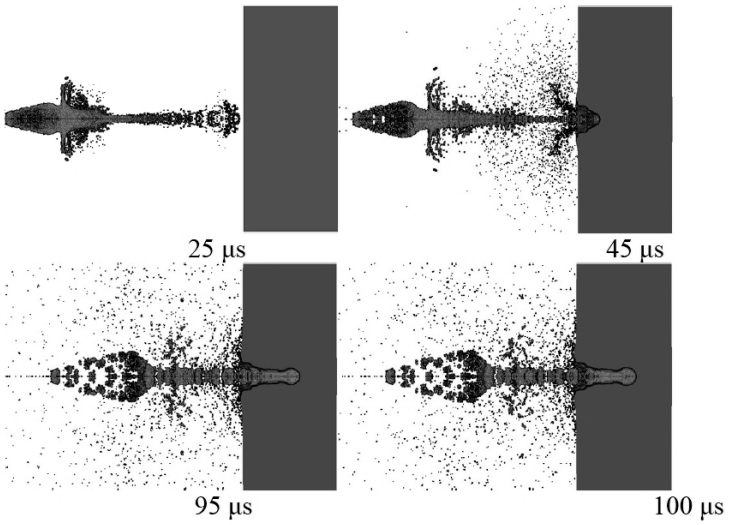

Fig. 9. PTFE/Cu particle jet penetrating the target plate process.

and the remaining velocity was high, so the damaged element continued to penetrate the target. After penetration 30 μs, the penetration depth increased only 3.3 mm, and finally reached 30.3 mm; while PTFE/Cu particle jet almost lost its penetrating depth. Because the head diameter of PTFE/Cu particle jet was larger than PTFE particle jet, and the accumulation of perforation in PTFE/Cu particle jet was more obvious, the perforation diameter of PTFE/Cu particle jet was 19.6 mm, which was 2.2 mm higher than PTFE particle jet. The maximum penetration depth of PTFE/Cu particle jet was 30.3 mm.

3.2. ***Penetration Performance Analysis***. From the numerical simulation results, we can see that the process of particle jet penetrating the target plate can be divided into three stages: pit opening stage, quasi-steady penetration stage and penetration termination stage. The results of numerical simulation showed that the process of particle material jet penetrating the target plate was consistent with the general law. From the start of detonating the shape charge, the particle jet passed through the forming and stretching process, and moved to the target plate and began to penetrate the target plate.

The results of numerical simulation showed that the head velocity of particle jet decreased rapidly when it reached the target plate during the pit-opening stage, and the energy of the pit opening was mainly derived from the material of the particle jet head. The PTFE particle jet began to penetrate the target plate at 6680 m/s at 24 μs, and then completed the pit opening after 11 μs. The PTFE/Cu particle jet began to penetrate the target plate at a velocity of 6102 m/s at 25 μs, and then completed the pit opening at the time of 29 μs. At the time of 29 μs, the jet began to penetrate the target plate at a velocity of 5263 m/s and completed the hole opening at 3 μs.

It can also be seen that the pit opening time of PTFE and PTFE/Cu jets is much longer than that of Cu jet. This was due to the fact that the head of PTFE and PTFE/Cu jets were not condensed, resulting in the dispersion of energy during the opening of pits. At the same time, its density was much less than that of Cu penetration ability, so the opening time was prolonged. Since then, because of the continuous impact of high velocity of subsequent particle jet on the target plate, the target material had also been impacted and eroded into the quasi-steady penetration stage, and as the penetration deepens, with the further decrease of particle jet velocity, the particle jet gradually lost its penetration ability, and the piling phenomenon occurred, which led to the end of penetration. At 70 μs, there was obvious jet accumulation phenomenon in PTFE particle jet. The penetration ability of the jet particles

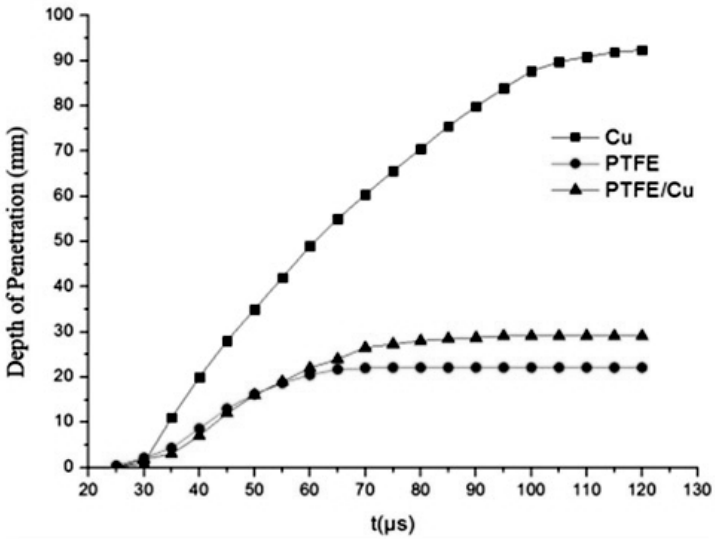

Fig. 10. Penetration depth variation curves of three materials particle jets penetrating target.

is weakened and accumulate in the penetration channel, when the maximum penetration depth is 22.1 mm. At 85 μs, there was obvious particle jet accumulation phenomenon in PTFE/Cu particle jet, and the maximum penetration depth was 29.1 mm; at 110 μs, there was an obvious accumulation of Cu particle jet, and the maximum penetration depth was 92.4 mm. The penetration depth of the three jets was shown in Fig. 10.

3.3. ***Penetration Experimental Verification***. It is a complex reaction process for particle jet damage elements to penetrate the target plate. Numerical simulation could not completely describe the real situation, in order to obtain a more realistic penetration effect, an experimental study on the penetration of 45# steel armor by particle jet damage elements formed by three different materials under explosive loading was carried out. Different materials particle jets penetration target plate are shown in Fig. 11. The penetration depth of Cu particle jet was 97.5 mm, the perforation aperture was 12.1 mm; PTFE particles flow penetration depth was 19.0 mm, perforated aperture was 18.3 mm; the modified PTFE particle jet penetration depth was 27.7 mm and the perforation aperture was 20.6 mm. The experimental results were in good agreement with the numerical simulation. Cu particle jet penetration results, PTFE particle jet penetration results, and PTFE/Cu particle jet penetration results are shown below.

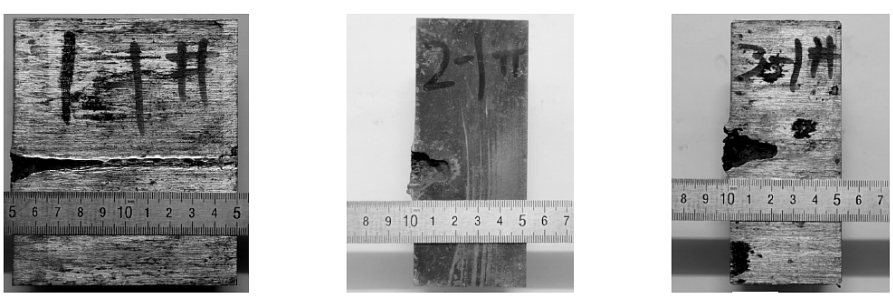

a b c

Fig. 11. Target plate penetration by particle jets from different materials: (a) Cu; (b) PTFE; (c) PTFE/Cu.

Conclusions

1. In this study of particle jets from three different materials, the numerical simulation and X-ray observations revealed that Cu, PTFE, and PTFE-Cu liners can form a particle jet damage element with a good shape. The Cu particle jet was compact, that of PTFE was evacuated, while the PTFE/Cu particle jet had the largest penetration diameter. The head velocity of Cu particle jet damage element was the lowest, that of PTFE was the highest, while that of PTFE/Cu particle jet was intermediate.

2. The head diameters of PTFE/Cu and PTFE particle jet damage elements were 3 and 2.7 mm, respectively. Thus, the PTFE/Cu particle jet had the best reaming ability of the target penetration, which was favorable for opening up the channel for the rear stage in the tandem shape charge.

3. Study on the penetration performance of PTFE particle jet in three different materials, the penetration depth of PTFE particle jet damage element to 45# steel was 19.0 and 27.7 mm for PTFE/Cu particle jet, the penetration depth of PTFE/Cu damage element was 45.8% higher than that of PTFE particle jet; the perforation diameter of PTFE particle jet was 18.3 mm, the perforation diameter of PTFE/Cu particle jet was 20.6 mm, and the perforation diameter of the PTFE/Cu increased by 12.6%, as compared to that of the PTFE particle jet, which shows that PTFE/Cu particle jet damage element has the highest damage performance.

Acknowledgments. The authors would like to acknowledge the financial support from the Project supported by the National Natural Science Foundation of China under Grant No. 11572291 and Talent Project of Joint Cultivation Base for Postgraduate Students in Shanxi Province No. 20160033.

1. W. Cai, *Study on Warhead Separation Technology*, Nanjing University of Technology (2008).
2. J. P. Yin and Z. J. Wang, *Ammunition Theory*, Beijing Institute of Technology Press, Beijing (2014).
3. C. Y. Hong, *New Advanced Technology of Ordnance Industry*, Ordnance Industries Press (1994).
4. M. Held, "Liners for shaped charges," *J. Battlefield Technol.*, **4**, No. 3, 1–7 (2001).
5. D. Alistar, "Some metallurgical aspects of shaped charge liners," *J. Battlefield Technol.*, 1, No. 1, 1–3 (1998).
6. B. H. Chang, J. P. Yin, Z. Q. Cui, and T. X. Liu, "Numerical simulation of modified low-density jet penetrating shell charge," *Int. J. Simul. Model.*, **14**, No. 3, 426–437 (2015).
7. M. Held, *Initiation Criteria of High Explosives, Attacked with Projectiles of Different Densities*: 27th International Annual Conference of ICT (June 25–28, 1996, Karlsruhe, Germany), TDW (1996).
8. Z. M. Guo and M. B. Liu, "Mechanism research of shaped charge jet with SPH," *Ordnance Mater. Sci. Eng.*, **36**, No. 4, 37–40 (2013).
9. P. J. König and F. J. Mostert, "The design and performance of non-initiating shaped charges with granular jets against ERA," in: Proc. of the 20th Int. Symp. on Ballistics (September 23–27, 2002, Orlando, FL), Vol. 2, DEStech (2002), pp. 858–863.
10. R. Cornish, J. T. Mills, J. P. Curtis, and D. Finch, "Degradation mechanisms in shaped charge jet penetration," *Int. J. Impact Eng.*, **26**, No. 1, 105–114 (2001).
11. R. J. Li, Z. W. Shen, and T. S. Liu, "Deep penetration mechanism of jet produced by shaped charge with porous liner at low-standoff distance," *Chinese J. Energ. Mater. (Hanneng Cailiao)*, **16**, No. 4, 424–427 (2008).

12. R. J. Li, *Study on the Jet Mechanisms of Shaped Charge with Porous Liner and Its Applications*, University of Science and Technology of China (2008).
13. M. B. Liu, G. R. Liu, Z. Zong, and K. Y. Lam, "Computer simulation of high explosive explosion using smoothed particle hydrodynamics methodology," *Comput. Fluids*, **32**, No. 3, 305–322 (2003).
14. L. Li, "Application of SPH method in 3D numerical simulation of charged charge jet," *Explos. Shock Waves*, **32**, No. 3, 316–322 (2012).
15. Y. B. Liu, *The Mechanism of Formation and Penetration of Shaped Charge Particle Jets*, University of Science and Technology of China (2012).
16. J. Chen, J. P. Yin, Y. Y. Han, et al., "Numerical simulation of low density particle jets formation based on SPH method," *Chinese J. Energ. Mater. (Hanneng Cailiao)*, **25**, No. 9, 756–762 (2017).

Received 15. 03. 2018